ARTICLE
Journal of Cellular Biochemistry 106:139–151 (2009)

Journal of Cellular Biochemistry

Prp45 Affects Prp22 Partition in Spliceosomal Complexes and Splicing Efficiency of Non-Consensus Substrates

Ondřej Gahura, Kateřina Abrhámová, Michal Skružný, Anna Valentová, Vanda Munzarová, Petr Folk, and František Půta*

Faculty of Science, Department of Cell Biology, Charles University in Prague, Prague 128 00, Czech Republic

ABSTRACT

Human transcription co-regulator SNW1/SKIP is implicated in the regulation of both transcription elongation and alternative splicing. Prp45, the SNW/SKIP ortholog in yeast, is assumed to be essential for pre-mRNA processing. Here, we characterize *prp45*(1–169), a temperature sensitive allele of *PRP45*, which at permissive temperature elicits cell division defects and hypersensitivity to microtubule inhibitors. Using a synthetic lethality screen, we found that *prp45*(1–169) genetically interacts with alleles of NTC members *SYF1*, *CLF1/SYF3*, *NTC20*, and *CEF1*, and 2nd step splicing factors *SLU7*, *PRP17*, *PRP18*, and *PRP22*. Cwc2-associated spliceosomal complexes purified from *prp45*(1–169) cells showed decreased stoichiometry of Prp22, suggesting its deranged interaction with the spliceosome. In vivo splicing assays in *prp45*(1–169) cells revealed that branch point mutants accumulated more pre-mRNA whereas 5′ and 3′ splice site mutants showed elevated levels of lariat-exon intermediate as compared to wild-type cells. Splicing of canonical intron was unimpeded. Notably, the expression of Prp45(119–379) in *prp45*(1–169) cells restored Prp22 partition in the Cwc2-pulldowns and rescued temperature sensitivity and splicing phenotype of *prp45*(1–169) strain. Our data suggest that Prp45 contributes, in part through its interaction with the 2nd step-proofreading helicase Prp22, to splicing efficiency of substrates non-conforming to the consensus. J. Cell. Biochem. 106: 139–151, 2009.

KEY WORDS: pre-mRNA PROCESSING; *SACCHAROMYCES CEREVISIAE*; Prp45; Prp22; SNW1/SKIP

Introns are recognized and spliced out of pre-mRNA through specific sequences in *cis*. The splicing signals are interpreted and complemented by the spliceosome, which is capable of transducing inputs from inside and outside of the cell into the changes of catalytic efficiency and splice site choice. Spliceosome assembles on a template in a still disputed series of associations and conformational changes of U1, U2, and U5.U4/U6 snRNP particles [Jurica and Moore, 2003; Valadkhan, 2005; Will and Luhrmann, 2006]. Before the first transesterification can occur, the U5.U4/U6 tri-snRNP containing complex, denoted B [Makarov et al., 2002], must be rearranged, releasing U1 and then U4 snRNPs and binding the Prp19 associated complex [Tarn et al., 1994]. This complex, named the CDC5L complex in metazoans and the NineTeen Complex (NTC) in *Saccharomyces cerevisiae*, supplies essential factors to the spliceosome and marks the transition from the inactive spliceosome B to the catalytically competent species [Ohi et al., 2005]. After the first transesterification, the spliceosome attains a conformation supporting the second step reaction [Mayas et al., 2006; Liu et al., 2007] in a process which requires the ordered recruitment of helicases and auxiliary 2nd step factors [James et al., 2002]. Helicases are indispensable also for the release of mRNA and of the intron lariat from the post-catalytic spliceosome [Arenas and Abelson, 1997].

Splicing in *S. cerevisiae* does not include an alternative selection of splice sites or complex SR protein interactions of metazoan cells [Shen and Green, 2006]. New results on regulated meiotic splicing [Juneau et al., 2007], on the gene-selective impacts of splicing factor

Ondřej Gahura and Kateřina Abrhámová contributed equally to this work.

Additional supporting information may be found in the online version of this article.

Grant sponsor: Czech Ministry of Education, Youth and Sports; Grant numbers: MSM0021620858, LC07032; Grant sponsor: Czech Science Foundation; Grant number: 204/02/1512; Grant sponsor: Grant Agency of the Charles University; Grant number: B170/2005.

Michal Skružný's present address is EMBL, Cell Biology and Biophysics Unit, Meyerhofstraße 1, 69117 Heidelberg, Germany.

Vanda Munzarová's present address is Institute of Microbiology, Academy of Sciences of the Czech Republic, Vídeňská 1083, 142 20 Praha 4, Czech Republic.

*Correspondence to: František Půta, Faculty of Science, Department of Cell Biology, Charles University in Prague, Praha 2, Viničná 7, Prague 128 00, Czech Republic. E-mail: puta@natur.cuni.cz

Received 17 July 2008; Accepted 8 October 2008 • DOI 10.1002/jcb.21989 • 2008 Wiley-Liss, Inc.

Published online 17 November 2008 in Wiley InterScience (www.interscience.wiley.com).

mutants [Pleiss et al., 2007b], or on the role of exon sequences in determining splicing efficiency [Crotti et al., 2007] suggest, however, that the "decision-algorithms" of the yeast spliceosome are very complex and subject to cellular regulation [Pleiss et al., 2007a]. These as well as earlier data on cell cycle-arrest phenotypes of splicing factor mutants [Burns et al., 2002] imply that the spliceosome differentiates among substrates and that facultative interactions take place on different pre-mRNA templates [Preker et al., 2002; Pleiss et al., 2007b]. It is perhaps because of this complexity that the yeast spliceosome has kept its many components, most of which have homologs in human [Stevens et al., 2002].

The human transcription co-regulator SNW1/SKIP is remarkable for the diversity of pathways in which it participates. It is involved in signaling by nuclear hormone receptors, E2F/pRb, CBF1/Notch, or TGFβ/Smad2, among others [Zhou et al., 2000; Leong et al., 2001; Zhang et al., 2001; Prathapam et al., 2002]. More recently, it was implicated in the regulation of elongating RNAPolII via P-TEFb and it was found to affect the production of alternative transcripts of several HIV genes [Bres et al., 2005]. Proteomic analyses confirmed the inclusion of SNW1/SKIP in the catalytically competent spliceosomal complexes and the post-spliceosomal species [Makarov et al., 2002; Bessonov et al., 2008]. The expression of a truncated SNW1/SKIP led to the accumulation of unspliced transcripts derived from a SKIP co-regulated reporter, indicating that SNW1/SKIP influences pre-mRNA splicing [Zhang et al., 2003].

Unlike SNW1/SKIP, its yeast ortholog *PRP45* was found, so far, to relate solely to splicing. Prp45 was identified in preparations of TAP-tagged Cef1, Prp19, Cwc2, Syf1, Yju2, Clf1/Syf3, and Prp46 [Gavin et al., 2002; Ohi and Gould, 2002], thus suggesting its partition in the NineTeen Complex. It associated with U2, U5, and U6 snRNP under nonsplicing conditions and with assembled spliceosomal complexes throughout the splicing process. In a two-hybrid screen, it interacted with the WD protein Prp46 and the DEAH-box helicase Prp22. The depletion of Prp45, which stalled cell growth, correlated with the accumulation of unprocessed pre-mRNA probes, irrespective of their BS-3′ss distance [Albers et al., 2003].

Here, we characterize a novel deletion mutant of the essential splicing factor *PRP45* (*prp45*(1–169)), which elicits cell cycle related defects and temperature dependent growth arrest. We found that Cwc2-purified spliceosomal complexes of the mutant are significantly depleted of Prp22 and that the mutant's ability to splice several non-consensus *ACT1-CUP1* substrates is grossly impaired. Furthermore, we documented that the *prp45*(1–169) deletion is synthetically lethal with alleles of the second step splicing factors *SLU7*, *PRP17*, *PRP18*, and *PRP22*, and of the NTC components *SYF1*, *CLF1*/*SYF3*, *NTC20*, and *CEF1*. We hypothesize that the C-terminal half of Prp45 aids in recruiting Prp22 to the spliceosome and is important for splicing of atypical introns.

MATERIALS AND METHODS

YEAST STRAINS AND PLASMIDS CONSTRUCTIONS

The *S. cerevisiae* strains used in this study are listed in Table I. The cultures were grown in supplemented SD, YPD, or YPAD media. The strains KAY01, KAY02, TSY01, and TSY02 were generated by PCR with pFA6a-3HA-kanMX6 [Longtine et al., 1998] replacing the *PRP45* coding sequence for amino acids 170 to 379 in the strains W303-1a, EGY48, KGY823, and KGY2914, respectively. WT and *prp45*(1–169) strains expressing GFP-tagged Tub1 or Cbf5 were obtained by crossing KAY02 with TUB1-GFP or CBF5-GFP strains, respectively, and selecting haploids carrying the relevant markers. The *prp45*(1–169) *dbr1*-Δ strain FPY2D was prepared as a progeny of B04999 and KAY02 crossing.

The plasmids pHIS-PRP45, pLexA-PRP45, pHIS-PRP45(1–190), p416ADH-PRP45(53–190), and pHIS-PRP45(170AAA) were described previously [Martinkova et al., 2002]. To obtain pADH416-PRP45(1–168), an *Eco*RI–*Pst*I fragment corresponding to amino acids 1–168 of Prp45 was cloned under the control of *ADH1* promoter. The fragments encoding Prp45(119–379),

TABLE I. Yeast Strains Used in This Study

Strain	Genotype	Source or reference
20376	*MAT***a**/α *his3-Δ1/his3-Δ1 leu2-Δ0/leu2-Δ0 ura3-Δ0/ura3-Δ0 lys2-Δ0/LYS2 MET15/met15-Δ0 prp45-Δ0::kanMX4/PRP45*	Res-Gen™, Invitrogen
W303-1a	*MAT***a** *ura3-1 leu2-3,112 trp1-1 his3-1,115 ade2-1 can1-100*	[Thomas and Rothstein, 1989]
KAY01	*prp45*(1-169)-*HA*:: *kanMX6*, otherwise as W303-1a	This study
EGY48	*MAT*α *his3 trp1 ura3 LexA*$_{op(x6)}$-*LEU2*	[Golemis et al., 1996]
KAY02	*prp45*(1-169)-*HA*::*kanMX6*, otherwise as EGY48	This study
FPY4B	*MAT***a** *prp45*(1-169)-*HA*::*kanMX6 ade2 ade3 his3 ura3 leu2* (pHT4467Δ-PRP45)	This study
AVY11	*MAT*α *prp45*(1-169)-*HA*::*kanMX6 ade2 ade3 his3 ura3 leu2 trp1* (pHT4467Δ-PRP45)	This study
B04999	*MAT***a** *dbr1-Δ::kanMX4 his3-Δ1 leu2-Δ0 ura3-Δ0 met15-Δ0*	Euroscarf
FPY2D	*MAT*α *prp45*(1-169)-*HA::kanMX6 dbr1-Δ::kanMX4 his3 ura3 leu2 trp1 met15*	This study
JBα	*MAT*α *ura3 leu2 his3 ade2 ade3*	[Bassler et al., 2001]
KGY823	*MAT***a** *ade2-101 leu2-Δ1 lys2-801 trp1-Δ1 ura3-52*	K. Gould
KGY1522	*MAT***a** *cef1-13 ade2-101 leu2-Δ1 lys2-801 trp1-Δ1 ura3-52*	K. Gould
KGY2818	*MAT***a** *prp17/cdc40-Δ his3-Δ1 leu1-Δ0 met15-Δ ura3-Δ0*	K. Gould
KGY2847	*MAT***a** *prp22-1 ade2 his3 ura3*	K. Gould
KGY2914	*MAT***a** *tub1Δi ade2-101 leu2-Δ1 lys2-801 trp1-Δ1 ura3-52*	K. Gould
TSY01	*prp45*(1-169)-*HA*::*kanMX6*, otherwise as KGY823	This study
TSY02	*prp45*(1-169)-*HA*::*kanMX6*, otherwise as KGY2914	This study
YDF53	*MAT***a** *ura3 leu2 his3 lys1, ade2 ade3 trp1 slu7::TRP1* (*URA3 SLU7* plasmid)	K. Guthrie
CWC2-TAP	*MAT***a** *CWC2-TAP*::*HIS3MX6 his3Δ1 leu2Δ0 met15Δ0 ura3Δ0*	[Ghaemmaghami et al., 2003]
CBP5-GFP	*MAT***a** *CBP5-GFP*::*HIS3MX6 his3Δ1 leu2Δ0 met15Δ0 ura3Δ0*	[Huh et al., 2003]
TUB1-GFP	*MAT***a** *TUB1-GFP*::*HIS3MX6 his3Δ1 leu2Δ0 met15Δ0 ura3Δ0*	[Huh et al., 2003]

Prp45(53–379), and Prp45(258–379) were generated by PCR, cut by *Eco*RI and *Xho*I, and inserted into p416ADH or pLexA. The plasmid pHIS-PRP45(Δ163–173) expressing Prp45 with the AAA substitution for the amino acids WKIPAAVSNW was obtained using the Altered Sites® II in vitro Mutagenesis System (Promega). In two sequential mutagenesis reactions the substitutions SNW170-172AAA and WKI163-165AAA were prepared and the sequence between *Not*I sites introduced in the reactions was eliminated. To construct the pHT4467Δ-PRP45, *PRP45* was PCR amplified and inserted as an *Xba*I–*Not*I fragment into the pHT4467Δ [Bassler et al., 2001]. pRS313-SLU7 was constructed by inserting the 3.3 kb *Bam*HI–*Sal*I fragment of *SLU7* locus into pRS313. The 5.5 kb *Sal*I–*Xba*I fragment containing *CLF1/SYF3* was inserted into a pRS313 vector to generate pRS313–CLF1. The plasmids pRS313-SLU7(P268L) and pRS313-SLU7(K252E) were prepared using DNA fragments obtained by PCR; DNA isolated from mutant strains FPY4B#2 and FPY4B#16 served as a template. To construct p413ADH-PRP22, the ORF of *PRP22* was PCR amplified and cloned as *Bam*HI–*Sal*I fragment into p413ADH.

SYNTHETIC LETHALITY SCREEN

The strains FPY4B and AVY11, used in the synthetic lethality (SL) screen, were prepared as a progeny of KAY01 and JBα [Bassler et al., 2001] crossing. The temperature-sensitive spore clone carrying the relevant markers was selected and transformed with pHT4467Δ-PRP45. The SL screen was performed as previously described [Koren et al., 2003]. The cells were UV irradiated in ca 2 mm layer of water suspension (Stratalinker; 254 nm, 15–25 mJ/cm^2) to obtain 2–10% survival. YEp13-based genomic library [Reed et al., 1989] was used to identify mutated genes.

ANALYSES OF PROTEIN COMPLEXES

PRP45 and *prp45*(1–169) strains expressing Cwc2-TAP fusion protein were used for tandem affinity purification (TAP) experiments. *CWC2-TAP prp45*(1–169) strain was obtained as a G418-resistant, *HIS*+, temperature sensitive progeny of KAY02 and CWC2-TAP strain crossing. Inoculum (50 ml) was grown in selective media, transferred to 2 L of YPD and cultivated for 6–8 generations to OD (600 nm) ~4.0. Cells were then collected, washed and frozen in liquid nitrogen. Cell lysis and TAP-purification were then performed essentially as described [Puig et al., 2001; Lopez de Heredia and Jansen, 2004]. Protein complexes were resolved by SDS–PAGE using 4–12% gradient gel (Invitrogen) and stained with Brilliant Blue G (Sigma). Selected bands were excised and processed by MALDI-TOF mass spectrometry identification. For Western blot analyses, anti-Prp22 (rabbit polyclonal; a gift from B. Schwer), anti-TAP (anti-CBP rabbit polyclonal; Open Biosystems), and anti-HA (mouse monoclonal, Babco) primary antibodies, and anti-rabbit and anti-mouse horse radish peroxidase conjugated secondary antibodies (BIORAD) were used. The immunoblot signal was visualized by the ECL chemiluminescence system (Amersham).

RNA ISOLATION AND PRIMER EXTENSION ANALYSIS

Cells transformed with plasmid pMM1C, pMM4C, pMA2C, pMA42, pCQ04, or pC256A expressing *ACT1-CUP1* fusion construct under the control of *TDH3* promoter [Lesser and Guthrie, 1993] were grown in SD medium to OD (600 nm) ~0.5–0.8. The cells were then harvested and total RNA was isolated by hot phenol extraction. The extension reactions were primed using the oligonucleotide YAC6, complementary to the proximal part of *CUP1* [Siatecka et al., 1999], or U1OG (5′-CGCCGTATGTGTGTGTGACC-3′), complementary to U1 snRNA. Probes were radiolabeled on 5′ ends using T4 Polynucleotide Kinase (Promega) and [γ-^{32}P] ATP (3,000 Ci/mmol; MP Radiochemicals). The reverse transcription was performed with the RevertAid™ M-MuLV Reverse Transcriptase (Fermentas) and 3–10 μg of RNA substrate. The products were separated on 8% polyacrylamide/7 M urea gels and visualized by autoradiography.

RESULTS

IDENTIFICATION AND CHARACTERIZATION OF TEMPERATURE SENSITIVE ALLELE OF *PRP45*

In Prp45, amino acids 190–249 are 37% identical (75% similar) to human SKIP protein. Nevertheless, as we have demonstrated previously, truncated or mutated variants of Prp45, including Prp45(1–190) or Prp45(170AAA), supported wild-type growth of *prp45*-Δ haploids [Martinkova et al., 2002]. Here, we show that the truncation of 52 N-terminal amino acids is viable in Prp45(53–379)-, but lethal in Prp45(53–190)-expressing cells. The protein with more extensive N-terminal truncation, Prp45(119–379), failed to support growth. The absence of the invariant SNWKN motif (Prp45(Δ163–173)) was compatible with viability at both 30° and 37°C, but the C-terminal truncation that encompassed the SNWKN motif (Prp45(1–168)) caused lethality at 37°C (Fig. 1A). The growth rate of *prp45*-Δ cells expressing Prp45(1–168) under the control of an *ADH1* promoter steadily declined after the temperature shift and became negligible after ca 24 h (data not shown).

To study the cells expressing the temperature sensitive variant of Prp45 at physiological levels, we prepared a *prp45*(1–169)-*3HA::kanMX6* substitution at the *PRP45* locus, using primer directed homologous recombination in the strain EGY48. The resulting mutant cells (KAY02) stopped their growth in liquid culture 6 h after the transfer to a non-permissive temperature (Fig. 1B). The same results were obtained with the *prp45*(1–169)-*3HA::kanMX6* substitution in the strain W303-1a (KAY01; data not shown). The morphology of *prp45*(1–169) cells suggested a cell division defect; a high proportion of cells from an exponentially growing culture at 30°C displayed elongated and deformed shapes. Some of the buds were rod-like with the necks widened (Fig. 1C). We tested the *prp45*(1–169) (KAY02) strain for its response to various stressors and found that it was hypersensitive to microtubule polymerization inhibitors, nocodazole and carbendazim (Fig. 1D and data not shown). The strain was also found to be hypersensitive to cycloheximide, reflecting perhaps the fact that some of the mRNA products, for example, ribosomal proteins, were already limiting at 30°C.

Previously, *TUB1* and *TUB3* splicing defects were documented for *cef1-13*, *prp17*-Δ, *prp22-1*, and *prp16-2* alleles [Burns et al., 2002; Chawla et al., 2003]. Burns et al. suggested that it is the differential requirement of certain splicing factors for the processing of a subset of transcripts that causes cell cycle arrest. To test whether defective splicing of *TUB1* intron was responsible for the observed defect in

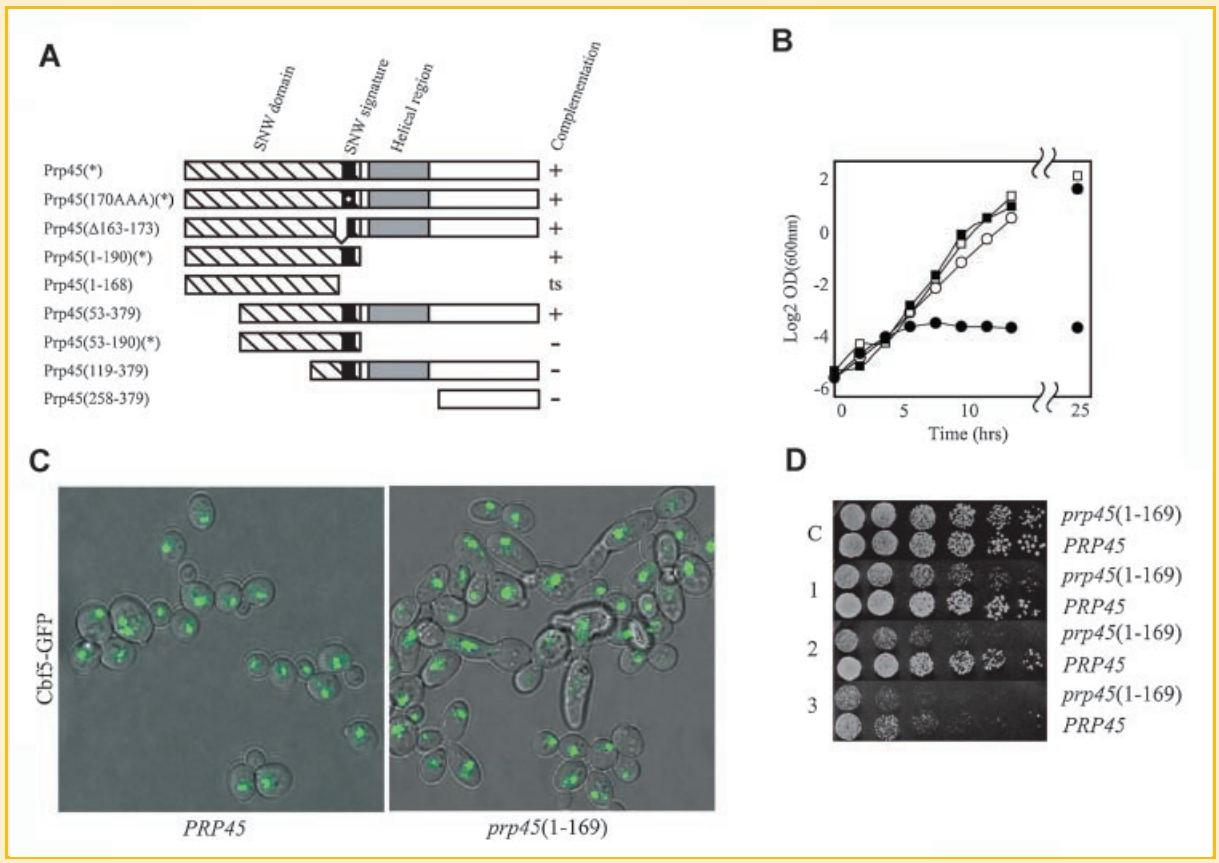

Fig. 1. Deletion analysis of *PRP45* identified a temperature sensitive allele *prp45*(1–169). A: Deletion analysis of *PRP45* delineates a region required for viability. *PRP45*/*prp45*-Δ strain was used to express either full-length Prp45 or its N-terminal, C-terminal or combined truncations or mutations under the control of an *ADH1* promoter. The cells were sporulated and individual spores tested for viability at 30°C, auxotrophy, and G418 resistance. The constructs indicated by asterisk (*) were published previously [Martinkova et al., 2002]. B: *prp45*(1–169) cells cease to grow after ca. 6 h of incubation at 37°C. *prp45*(1–169) (circles) and *PRP45* (squares) strains were cultivated in SD medium at 30°C (empty symbols) or 37°C (filled symbols). C: *prp45*(1–169) deletion leads to aberrant cell morphology. *prp45*(1–169) cells expressing chromosomally tagged Cbf5-GFP were grown at 30°C and observed under a Leica TCS SP2 confocal microscope (right panel). The Cbf5-GFP was used to visualize the nuclei (majority of the signal is localized in nucleoli). *PRP45 CBF5-GFP* cells were used as controls (left panel). D: *prp45*(1–169) cells exhibit hypersensitivity to nocodazole and cycloheximide. *prp45*(1–169) and *PRP45* cells were cultivated to a middle-log phase at 30°C, serially diluted in 1:3 ratios, spotted on YPAD plates (C) or YPAD plates containing 5 μg/ml nocodazole (1), 7.5 μg/ml nocodazole (2), or 0.04 μg/ml cycloheximide (3), and incubated for 1.5 day.

prp45(1–169) cells, we expressed the intronless *TUB1* gene (*tub1Δi*) and its WT version from a centromeric vector under the control of an autologous promoter [Burns et al., 2002] in *prp45*(1–169) and *PRP45* cells, and tested their growth ability at 30° or 37°C. The expression of intronless tubulin gene did not alleviate the growth defect to any extent (Fig. 2A). To further test the influence of *TUB1* intron deletion on the microtubule depolymerizing drug sensitive phenotype of the *prp45*(1–169) mutant, we generated *prp45*(1–169)-*3HA::kanMX6* substitutions in KGY2914 (*tub1Δi*) and KGY823 (*TUB1* WT) strains. The removal of *TUB1* intron from the genome only slightly restored the resistance of *prp45*(1–169) cells to nocodazole (Fig. 2B). In addition, when *prp45*(1–169) strain expressing GFP-tagged Tub1 under an autologous promoter was examined, cells with mitotic spindle structures were observed even after ca. 4 h incubation at 37°C (data not shown).

Microscopic examination of synchronized *prp45*(1–169) cells cultivated at 37°C confirmed the accumulation of large-budded cells arrested during the terminal stages of cell division (Fig. 2C). DAPI stained nuclear content appeared segregated to the mother and daughter cells, but there were no other buds forming on the doublets. The doublets were connected by Calcofluor-positive septa, some of which were already contiguous as judged by the examination of optical sections (data not shown).

prp45(1–169) IS SYNTHETICALLY LETHAL WITH MUTANT ALLELES OF NTC COMPONENTS AND SECOND STEP SPLICING FACTORS

prp45(1–169) cells grew at WT-rates at the permissive temperature, which suggested that splicing was not affected taken as a whole. We reasoned that such cells would be suitable for discriminatory genetic analysis of synthetic lethality. We employed a synthetic lethality screen with *prp45*(1–169) strain transformed with a pHT4467Δ-PRP45 plasmid (Fig. 3A). After UV mutagenesis, we obtained 39 candidate clones among which we found the mutants of *SLU7*, *PRP18*, *SYF1*, *CLF1/SYF3*, *NTC20*, *PRP22*, and *CEF1*. The list of the clones and genes identified by complementation and molecular nature of some of the mutations is presented in Table II. The

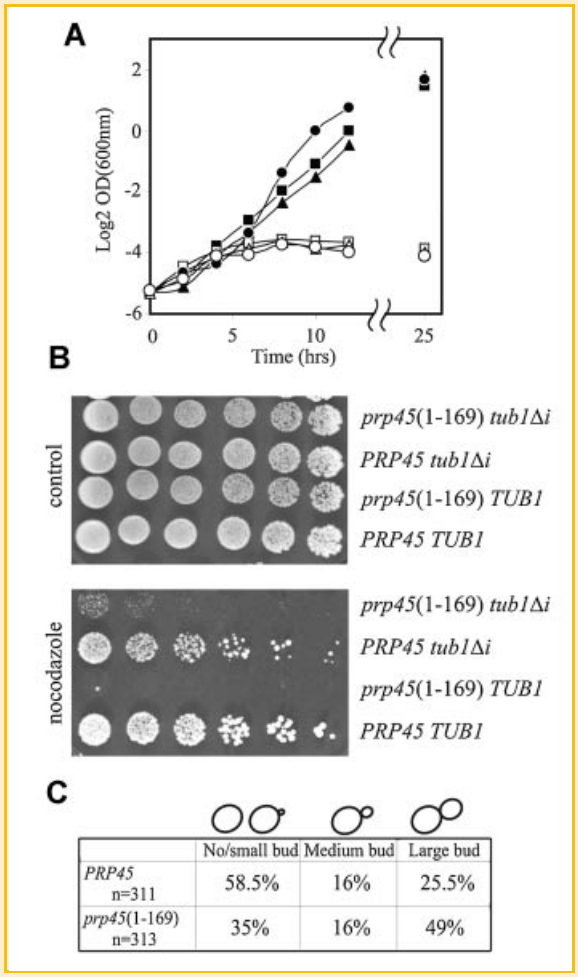

Fig. 2. The phenotype of *prp45*(1–169) cells cannot be assigned to the inefficiency of *TUB1* splicing. (A) Expression of tubulin α from either *TUB1* or intronless *tub1Δi* does not overcome the temperature sensitivity phenotype of *prp45*(1–169) cells. *prp45*(1–169) cells were transformed with pRS415-TUB1 (triangles), pRS415-tub1Δi (circles), or empty plasmid (squares) as a control. Transformants were grown in selective medium at 30°C (filled symbols) or 37°C (empty symbols). B: Excision of intron from *TUB1* does not eliminate the hypersensitivity of *prp45*(1–169) cells to nocodazole. Indicated strains were cultivated to a middle-log phase, serially diluted (ratio 1:3), and spotted on YPAD plates with or without 5 μg/ml nocodazole. The plates were incubated at 30°C for 3 days. C: Hydroxyurea-synchronized culture of the *prp45*(1–169) mutant accumulates large-budded cells at restrictive temperature. *prp45*(1–169) and *PRP45* cells were grown in YPAD medium at 30°C to OD (600 nm) ~0.3, synchronized at 37°C for 3 h in the presence of 15 mg/ml hydroxyurea, washed twice with water, and released into double volume of YPAD medium; both the water and the medium were preheated to 37°C. The cells were collected 3 h after the release, washed, stained by DAPI (1 μg/ml) or Calcofluor white (1 mg/ml) and analyzed under a confocal microscope. The percentage of cells with small (or absent), medium, or large buds was determined [Racki et al., 2000].

complementation experiments are illustrated in Figure 3B (left panel). We discuss in more detail the mutations of *SLU7*, *CLF1* (see below), and *PRP22* (see the next paragraph).

Slu7, which binds the spliceosome through U5 snRNP and the DExH-box protein Brr2, cooperates with Prp18 in the second step of splicing and is required for stage specific recruitment of Prp22 [van Nues and Beggs, 2001; James et al., 2002]. Sequencing of *slu7* alleles of the strains FPY4B#2 and FPY4B#16 revealed single missense mutations P268L and K252E, respectively. To prove that these mutations were responsible for the synthetic lethality, the corresponding alleles were inserted into a shuttle vector and their inability to rescue pHT4467Δ-PRP45 dependence of FPY4B#2 and FPY4B#16 strains was confirmed by plasmid shuffling (Fig. 3 B and C). Either allele proved functional in *slu7*-Δ background at all temperatures tested (Fig. 3C and data not shown). *slu7*(P268L) did not suppress the synthetic lethal interaction of *prp45*(1–169) with *slu7*(K252E) and vice versa (Fig. 3C). Both mutations map within a highly conserved region between amino acids 247 and 271, adjacent to the Prp18 binding area and within the essential part of the protein [Zhang and Schwer, 1997]. The sequence contains six invariant residues, one of which is replaced in the P286L mutation (Fig. 3D).

CLF1/SYF3 was originally identified in a synthetic lethality screen with *prp17*-Δ [*CDC40*; Ben Yehuda et al., 2000] and forms part of the protein–protein interaction network of the NineTeen Complex [Ohi and Gould, 2002]. Clf1 protein consists of two super helices coiled of tetratricopeptide repeat units (TPR) and a partly conserved C-terminal region. The N- and C-terminal super helix interacts, among other factors, with Cef1 and Syf2, respectively, while the non-TPR region binds Prp22 [Ben Yehuda et al., 2000]. The TPR motifs are not interchangeable and their deletions show allele specific genetic interactions with, for example, *prp22* or *cwc2* alleles [Vincent et al., 2003]. Analysis of the strain FPY4B#3 revealed a *clf1* allele bearing mutations T402I and S404F. The genetic link between *prp45*(1–169) and *clf1*(T402I,S404F), which contains missense mutations within the TPR motif 11, might reflect a novel TPR motif-specific interaction of Clf1.

To complement the SL screen results, several previously characterized temperature sensitive mutants of splicing factors were also scored for synthetic lethality with *prp45*(1–169). The *prp45*(1–169) strain harboring plasmid-born *PRP45* was crossed with the candidate mutant strain and the diploid obtained was sporulated. The synthetic lethal relationship was then tested by plasmid shuffling (see Fig. 3B, right panel). Among the mutants analyzed, *prp22-1*, *cef1-13*, and *prp17*-Δ alleles were found to be synthetically lethal with *prp45*(1–169).

Prp45 AND Prp22 FUNCTIONALLY INTERACT

Our findings of the *prp45*(1–169) genetic partners and the results of previous proteomic [Ohi et al., 2002; Wang et al., 2003] and two-hybrid [Albers et al., 2003] analyses suggested that Prp45 is associated with NineTeen Complex components and with NTC activated spliceosome during both catalytic steps. We aimed to compare the protein composition of NTC associated complexes between WT and *prp45*(1–169) cells using tandem affinity purification (TAP). TAP-tagged Cwc2 was chosen as bait because it interacts with the WD40 domain of the tetrameric Prp19 core scaffold of the NineTeen Complex [Ohi and Gould, 2002].

Spliceosomal complexes from *CWC2-TAP PRP45* and *CWC2-TAP prp45*(1–169) strains were purified and analyzed by gradient PAGE. The protein bands were annotated based on pattern correspondence to available TAP datasets and the identity of

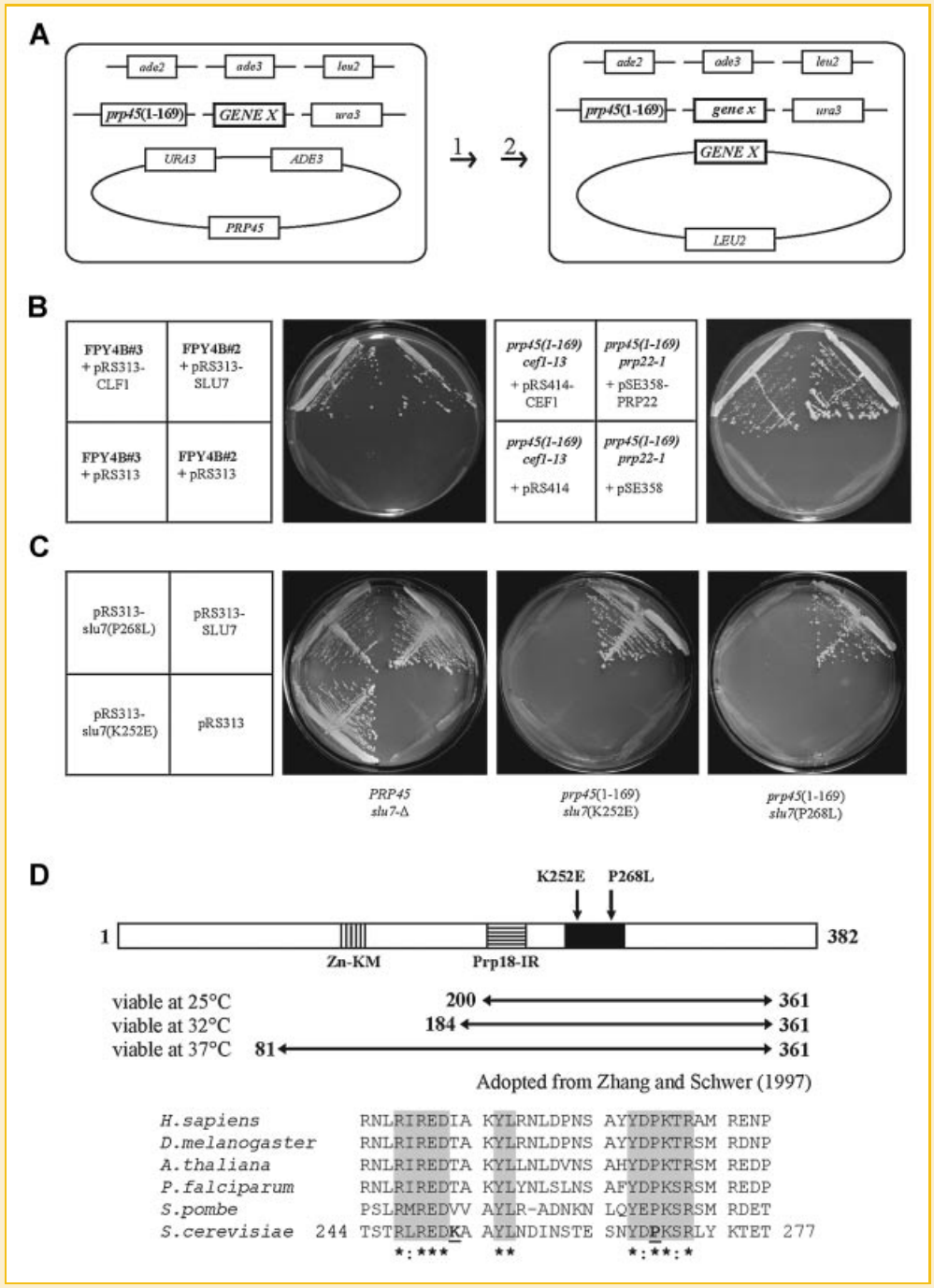

Fig. 3. *prp45*(1–169) is synthetically lethal with mutant alleles of NTC members and second step splicing factors. Scheme of synthetic lethal interaction testing. Cells harboring genomic *prp45*(1–169) and expressing Prp45 from a *PRP45 URA3 ADE3* plasmid (left panel) are subjected to UV radiation mutagenesis. When a mutation in a gene (*GENE X*) exhibits synthetic lethal interaction with *prp45*(1–169), the mutant cells become dependent on the *PRP45 URA3 ADE3* plasmid. Plasmid dependent cells form red non-sectoring colonies and are sensitive to 5-FOA (step 1). Their transformation with a plasmid bearing WT allele of the *GENE X* makes the *PRP45 URA3 ADE3* plasmid redundant and leads to its loss. The cells form 5-FOA resistant white colonies (step 2; right panel). B: Documentation of selected synthetic lethal interactions identified by UV mutagenesis and library screening (left panel) and by testing of previously characterized mutants of splicing factors (right panel). FPY4B#2 and FPY4B#3 cells were transformed with plasmids expressing *SLU7* and *CLF1*, respectively. Empty plasmid was used as a control. The transformants were tested for their ability to grow on media supplemented with 1 mg/ml 5-FOA (left panel). The strain *prp45*(1–169) *cef1-13* (pHT4467Δ-PRP45) was transformed with pRS414-CEF1 or empty pRS414 and tested for 5-FOA resistance. The same tests were done with the strain *prp45*(1–169) *prp22-1* (pHT4467Δ-PRP45) and the plasmids pSE358-PRP22 and pSE358 (right panel). C: Characterization of the novel *slu7* alleles. The strains *PRP45 slu7*-Δ (YDF53), *prp45*(1–169) *slu7*(P268L) (FPY4B#2), or *prp45*(1–169) *slu7*(K252E) (FPY4B#16) were transformed with the indicated plasmids, restreaked, and tested for their ability to grow on 5-FOA plates. D: slu7 mutations P268L and K252E map to a highly conserved C-terminal motif. The Slu7 diagram highlights the conserved regions and the amino acid substitutions identified in the *prp45*(1–169) SL screen (arrows). The regions required for viability at various temperatures are indicated [adopted from Zhang and Schwer, 1997]. The alignment of Slu7 proteins from selected organisms was constructed using ClustalW [Thompson et al., 1994]. The novel *SLU7* mutations are underlined; invariant and conserved residues are denoted by stars and colons, respectively.

TABLE II. Results of the Synthetic Lethality Testing of *prp45*(1–169)

Genes identified	Alleles	Isolate/strain number
UV mutagenesis library screen		
PRP22	*prp22*(300PPI)	AVY11#30
	prp22(-158T)	AVY11#28
	prp22(-327A)	AVY11#38
SLU7	*slu7*(P268L)	FPY4B#2
	slu7(K252E)	FPY4B#16
CLF1/*SYF3*	*clf1*(T402I,S404F)	FPY4B#3
	ND	AVY11#39
PRP18	ND	AVY11#43
SYF1	ND	AVY11#41
NTC20	ND	AVY11#36
CEF1	ND	AVY11#22
Test of previously characterized alleles		
PRP22	*prp22-1*	KGY2847
CEF1	*cef1-13*	KGY1522
PRP17	*prp17*-Δ	KGY2818

ND, not determined.

selected bands was confirmed by mass spectrometry. The comparison revealed a marked decrease of the quantity of Prp22 (migrating at 130 kDa) in the Cwc2-TAP pull-down from *prp45*(1–169). Western analysis using anti-Prp22 and anti-TAP specific antibodies confirmed this result (Fig. 4A).

Prp22 is an ATP dependent RNA helicase which is required for both the release of spliced mRNA from the spliceosome [Schwer and Gross, 1998] and, as part of a fidelity control mechanism, for the rejection of mutated/rate-limiting lariat-exon 2 intermediates [Mayas et al., 2006]. It was implicated in dislodging interactions between the pre-mRNA substrate and U5 snRNA [Aronova et al., 2007] and between exon 2 of the spliced mRNA and the spliceosome [Schwer, 2008]. We hypothesize that Prp45 is one of the proteins which are involved in the recruitment or regulation of the Prp22 helicase. We identified four alleles of *PRP22* as synthetically lethal with *prp45*(1–169) (see Table II). Two of them bear mutations in the 5′ non-coding region of the gene (*prp22*(-158T) and *prp22*(-327A)). Western analysis of Prp22 levels in these mutants revealed a marked decrease of Prp22 protein (Fig. 4B). One of the *PRP22* alleles,

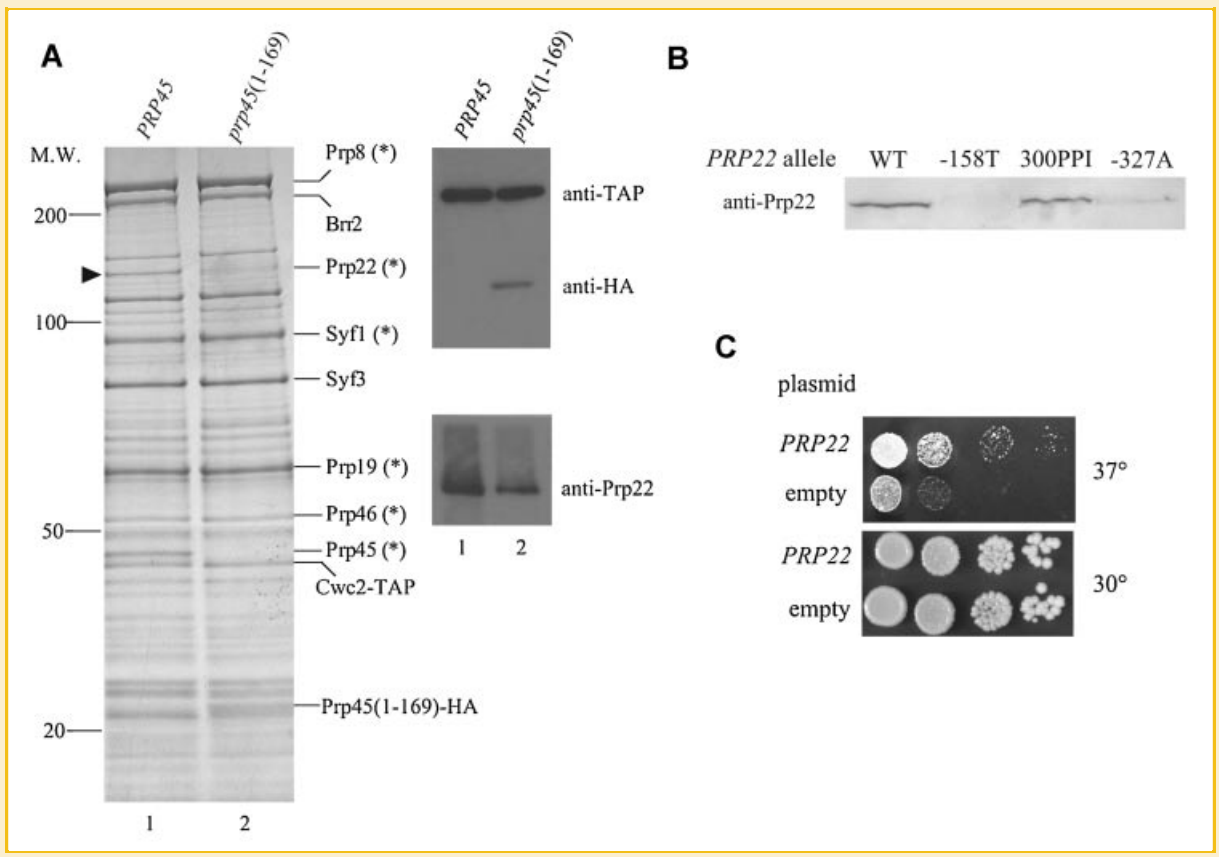

Fig. 4. Prp45 and Prp22 functionally interact. A: Deletion of the Prp45 C-terminus results in decreased stoichiometry of Prp22 in purified NTC associated complexes. Tandem Affinity Purification was used to isolate Cwc2-TAP complexes from *PRP45* (lane 1) and *prp45*(1–169) cells (lane 2) cultivated at 23°C. Proteins were separated on a 4–12% gradient SDS-PAGE and stained by colloidal Coommasie Brilliant blue (left panel) or analyzed by Western blotting using the indicated antibodies (right panels). Protein bands are labeled based on the pattern of published TAP data; the bands analyzed by mass spectrometry are indicated by asterisks. B: Cells harboring the alleles *prp22*(-158T) and *prp22*(-327A) show decreased concentration of Prp22 as compared to WT. Cultures were prepared in YPD medium to OD ~0.8 and harvested. Prp22 levels in samples of equal protein content were determined immunochemically. C: The over-expression of Prp22 partially suppresses temperature sensitivity of *prp45*(1–169) cells. The effect of temperature on the growth of *prp45*(1–169) cells transformed with 2 μm plasmid expressing WT Prp22 under the control of autologous promoter or with empty plasmid was compared. Both cultures were grown at 30°C to the same cell density (OD ~0.5) and 10-fold serial dilutions were spotted on YPD plates. The photographs were taken after 4 days of incubation at the indicated temperatures.

prp22(300PPI), bears R300P, Q301P, and L302I substitutions within a region which is N-terminal to the ATPase domain and necessary but not sufficient for spliceosome binding [Schneider and Schwer, 2001]. Finally, one *PRP22* allele was identified by direct testing; *prp22-1* harbors a G776E mutation in the inter-domain cleft of the catalytic domain of the ATPase [Arenas and Abelson, 1997]. Thus, both the mutations within the C-terminal half of Prp22, containing the ATPase/helicase domain, and within the N-terminal half are synthetically lethal with *prp45*(1–169). Notably, while both halves are required for functional spliceosome association, they also function when expressed *in trans* [Schneider and Schwer, 2001]. Our hypothesis is also supported by the finding that moderate over expression of Prp22 partly suppressed the ts phenotype of *prp45*(1–169) cells (Fig. 4C).

SPLICING DEFECTS OF INTRON MUTANTS ARE EXACERBATED IN *prp45*(1–169) CELLS

The genetic interactions of *prp45*(1–169) as well as the decreased stoichiometry of Prp22 in tandem affinity purified Prp45(1–169) containing spliceosomes led us to examine step-specific splicing defects using reporter templates in vivo [Liu et al., 2007]. We transformed the *prp45*(1–169) strain and the corresponding WT with plasmids expressing an *ACT1-CUP1* fusion construct containing mutations in the 5′ splice site, branch point, or the 3′ splice site region of the *ACT1* intron. Levels of pre-mRNA, lariat-exon 2 intermediate, and mRNA were analyzed using primer extension assay.

Splicing of the consensus template, that is, containing a canonical *ACT1* intron sequence, in *prp45*(1–169) strain proceeded with WT efficiency (Fig. 5A, lanes 1 and 3). Splicing appeared normal even in growth-arrested cells, that is, incubated at 37°C for up to 8 h (data not shown). The latter observation suggests that it is a defect limited to a subset of transcripts, rather than a generalized impairment of spliceosomal performance, that underlies the growth arrest phenotype of *prp45*(1–169) cells at 37°C. Splicing of a construct with U(-3) to G mutation of the 3′ss (gAG; Fig. 5A, lanes 2 and 4) was impaired only in the 2nd step. Splicing in cells cultivated at 37°C yielded similar results (data not shown). The gAG bearing reporter acts as less efficient 2nd step substrate and was used to map the properties of 2nd step acting factors, such as Prp22 [Mayas et al., 2006]. No effects on splicing efficiency were observed using 3′ss cAG or aAG reporters. *prp45*(1–169) strain derived from W303-1a gave essentially the same results as described above (data not shown).

Splicing of templates with mutated 5′ splice site residues in *prp45*(1–169) cells revealed that mainly the 2nd step defect was exacerbated. While *prp45*(1–169) apparently impaired splicing of a construct with A(+3) to C mutation of the 5′ss at both steps (A3C; Fig. 5B, lanes 1–4), the assay in *dbr1*-Δ background (*prp45*(1–169) *dbr1*-Δ) revealed that lariat-exon 2 intermediate was the primary accumulation product (Fig. 5B, lanes 2 and 4). A3C generates one

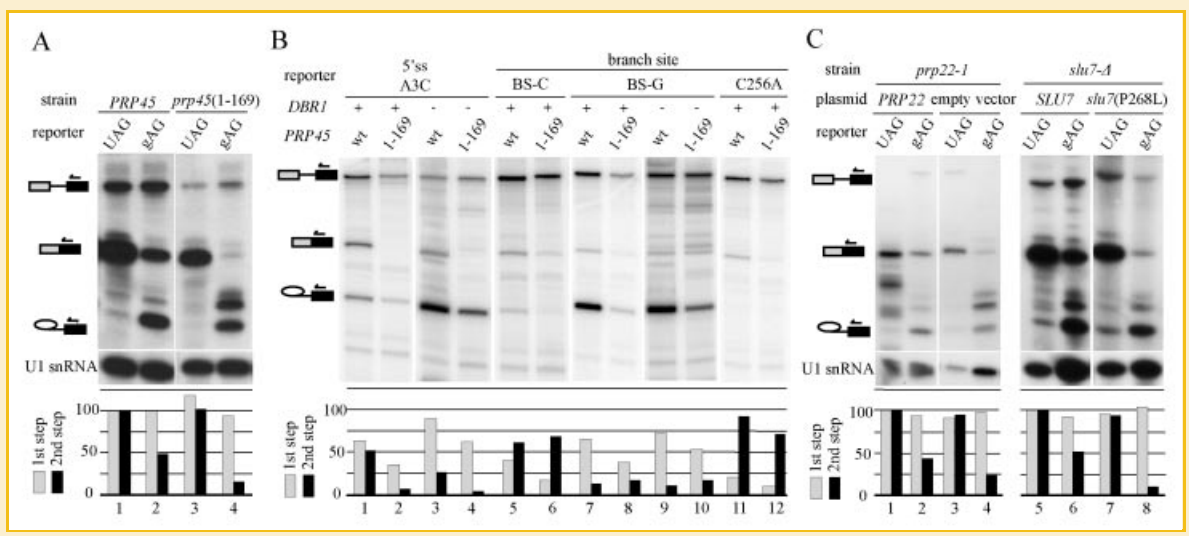

Fig. 5. Deletion of the Prp45 C-terminus decreases the splicing efficiency of non-canonical pre-mRNA templates. Cells expressing various *ACT1-CUP1* fusion constructs were grown at 30°C to a mid-log phase. RNA was isolated and subjected to primer extension analysis as described in Materials and Methods Section. The products corresponding to pre-mRNA (P), mRNA (M), and lariat-exon 2 intermediate (LI) are indicated by their icons. The signal appearing between M and LI bands in A and C was found to represent primer extension products of the endogenous *CUP1*/*CUP2* locus. U1 snRNA content was assayed as a control (A and C; bottom panels). For the construction of the bar diagrams, we used the phosphorimager signals from several independent experiments to quantify the apparent efficacies of the 1st (M + LI)/(P + M + LI) and 2nd step M/(M + LI). The values for each construct were normalized to the corresponding efficiencies of the consensus reporter in WT/control strain. A: *prp45*(1–169) impairs suboptimal 3′ splice site usage. *ACT1-CUP1* fusion constructs with UAG (WT; lanes 1 and 3) or gAG 3′ splice sites (lanes 2 and 4) were used. B: Suboptimal 5′ splice site and branch point sequences are spliced with lower than WT efficiency in *prp45*(1–169) cells. Splicing of *ACT1-CUP1* fusion constructs with mutated 5′ splice site (A3C; lanes 1–4) or branch site (BS-C, BS-G, or C256A; lanes 5–12) sequences was compared between WT and *prp45*(1–169) cells as indicated. Experiments in *dbr1*-Δ background were also included to account for the effect of debranching (lanes 3, 4, 9, and 10). C: *slu7*(P268L) and *prp22-1* exhibit gAG splicing defect similar to *prp45*(1–169). The left panel shows *prp22-1* strain harboring either Prp22 expressing plasmid or empty vector (lanes 1–4). The right panel documents splicing of *slu7*-Δ strain harboring plasmids expressing either WT Slu7 or Slu7(P268L) (lanes 5–8).

Watson-Crick pair in addition to the WT situation in the complex formed between U6 snRNA and the template after the rearrangement catalyzed by NTC [see Chan and Cheng, 2005]. This condition is interpreted as the hyper-stabilization of the first step conformation [see Konarska et al., 2006].

Splicing of branch point mutated templates in *prp45*(1–169) cells showed the exacerbation of the 1st but not the 2nd step defect (Fig. 5B, lanes 5–10). Assays were performed using a construct with branch site A to G mutation (BS-G), which is predominantly second step limiting, and A to C mutation (BS-C), which forms the lariat product inefficiently and is limiting for both steps. In cells lacking lariat debranching activity (*dbr1*-Δ), the accumulation of lariat-exon 2 intermediate through defective splicing was not attenuated by its removal, thus providing a more direct measure of the 2nd step efficiency (Fig. 5B, lanes 9–10). In addition, a branch site proximal C256A mutation, which destabilizes the first step conformation presumably because it pairs less efficiently with U2 snRNA [Smith et al., 2007], was tested. We found that *prp45*(1–169) exacerbated the first step defect associated with this substrate (Fig. 5B, lanes 11–12).

The mutants *slu7*(P268L) and *prp22-1* were tested for splicing using the same *ACT1-CUP1* reporter templates. *slu7*(P268L) markedly decreased the 2nd step efficiency with both gAG and A3C reporters, while *prp22-1* moderately exacerbated the 2nd step defect of the gAG substrate only (Fig. 5C and data not shown). The alleles did not affect splicing of branch point mutated reporters, in agreement with the documented role of both Slu7 and Prp22 in the 2nd step of splicing.

CO-EXPRESSION *IN TRANS* OF THE C-TERMINAL AND N-TERMINAL PARTS OF Prp45 RESTORES THE FUNCTIONALITY OF Prp45

Prp45 requires either of the termini for its essential function, as documented in strains dependent on Prp45(53–379) or Prp45(1–169). Truncation of both ends, however, yields a non-functional protein (Prp45(53–190); Fig. 1A). We asked whether the expression *in trans* of the C-terminal part of Prp45 in *prp45*(1–169) cells would affect the *prp45*(1–169) associated phenotypes. Indeed, the expression of Prp45(119–379) in *prp45*(1–169) cells eliminated their temperature sensitivity (Fig. 6A).

To test whether also the synthetic lethal interactions of *prp45*(1–169) would be suppressed by Prp45(119–379), we employed the respective double mutant strains harboring *PRP45* on a *URA3* plasmid and tested their 5-fluoroorotic acid (5-FOA) sensitivity in the presence of Prp45(119–379). Prp45(119–379) suppressed the synthetic lethal interaction of *prp45*(1–169) with *slu7*(P268L) or *slu7*(K252E) at 30°C as well as with *prp22-1* at 23°C. In other SL pairs however, Prp45(119–379) had only weak suppression capability (*clf1*(T402I,S404F)) or had no effect at all (*cef1-13*, *prp17*-Δ; Fig. 6B).

To assess whether the expression of Prp45(119–379) can complement *prp45*(1–169) phenotype at the biochemical level, we performed Cwc2-TAP purification of spliceosomal complexes from *prp45*(1–169) cells expressing Prp45(119–379) or WT Prp45. We observed that Prp45(119–379) restored the content of Prp22 in purified Cwc2-TAP complexes to the same levels as WT protein (Fig. 6C). This implies that the C-terminal part of Prp45 is required for proper interaction of Prp22 with the spliceosome and, at the same time, that it is structurally autonomous.

Finally, we asked whether splicing in *prp45*(1–169) cells expressing Prp45(119–379) reflects the restored partition of Prp22 in the Cwc2-TAP purified spliceosomes. The co-expression of Prp45(119–379) restored the splicing efficiencies of reporter templates to the levels observed in WT Prp45 co-expressing cells (Fig. 6D and data not shown), thus confirming that the expression *in trans* of Prp45(119–379) is sufficient to rescue the splicing phenotype of *prp45*(1–169).

DISCUSSION

THE PHENOTYPE OF *prp*45(1–169) CELLS IS INDEPENDENT ON *TUB*1 INTRON REMOVAL

We found that cells harboring the extensively truncated variant of Prp45 (Prp45(1–169)) display temperature sensitivity, shape defects and are hypersensitive to nocodazole (Fig. 1). Nocodazole sensitivity typically reflects changes in the stability and regulation of the microtubule network of the cell. In addition, defects in cell wall architecture, or deranged cell cycle regulations, which add strain to the functioning of the microtubule structures, also increase the sensitivity to microtubule polymerization inhibitors [see, e.g., Korolyev et al., 2005]. Alleles of several splicing factors such as *PRP17*, *PRP22*, or *CEF1* were shown to preferentially affect the splicing of *TUB1* intron, destabilizing microtubules and blocking cells at G2/M transition [Vijayraghavan et al., 1989; Shea et al., 1994; Vaisman et al., 1995]. The removal of intron from *TUB1* (*tub1Δi*) alleviated the block before entry to anaphase and partly restored the growth defect [Burns et al., 2002]. In *prp45*(1–169) cells, the temperature sensitivity as well as the levels of tubulin α protein were independent of *TUB1* intron removal (Fig. 2A and data not shown). We observed only a subtle increase in nocodazole resistance of *prp45*(1–169) *tub1Δi* cells compared to *TUB1* controls (Fig. 2B). Hydroxyurea synchronized *prp45*(1–169) mutant arrested with an increased proportion of large budded cells (Fig. 2 C), in which it resembled the behavior of the *cef1-13 tub1Δi* strain [Burns et al., 2002]. We reason that the phenotype of *prp45*(1–169) cells reflects changes in transcripts other than *TUB1* that are preferentially affected by the truncated Prp45. For example, inefficient splicing of suboptimal intron of the *ANC1* gene, which codes for a non-essential RNAPolII holo-complex associating factor [Kabani et al., 2005], was found responsible for temperature sensitive cell cycle arrest in *prp17*Δ cells [Dahan and Kupiec, 2002].

prp45(1–169) GENETICALLY INTERACTS WITH SPLICING FACTORS OF THE NTC-CONTAINING SPLICEOSOME

Using synthetic lethality testing, we identified genetic interactions between *prp45*(1–169) and alleles of *SLU7*, *PRP17*, *PRP18*, *PRP22*, *SYF1*, *CLF1/SYF3*, *NTC20*, and *CEF1*. All these SL partners belong to an extensive network of genetic and physical interactions, which was established for the NTC members and 2nd step-acting splicing factors. The essential splicing factor Cef1, which together with Snt309 and Cwc2 binds to the NTC scaffold protein Prp19 [Tsai et al.,

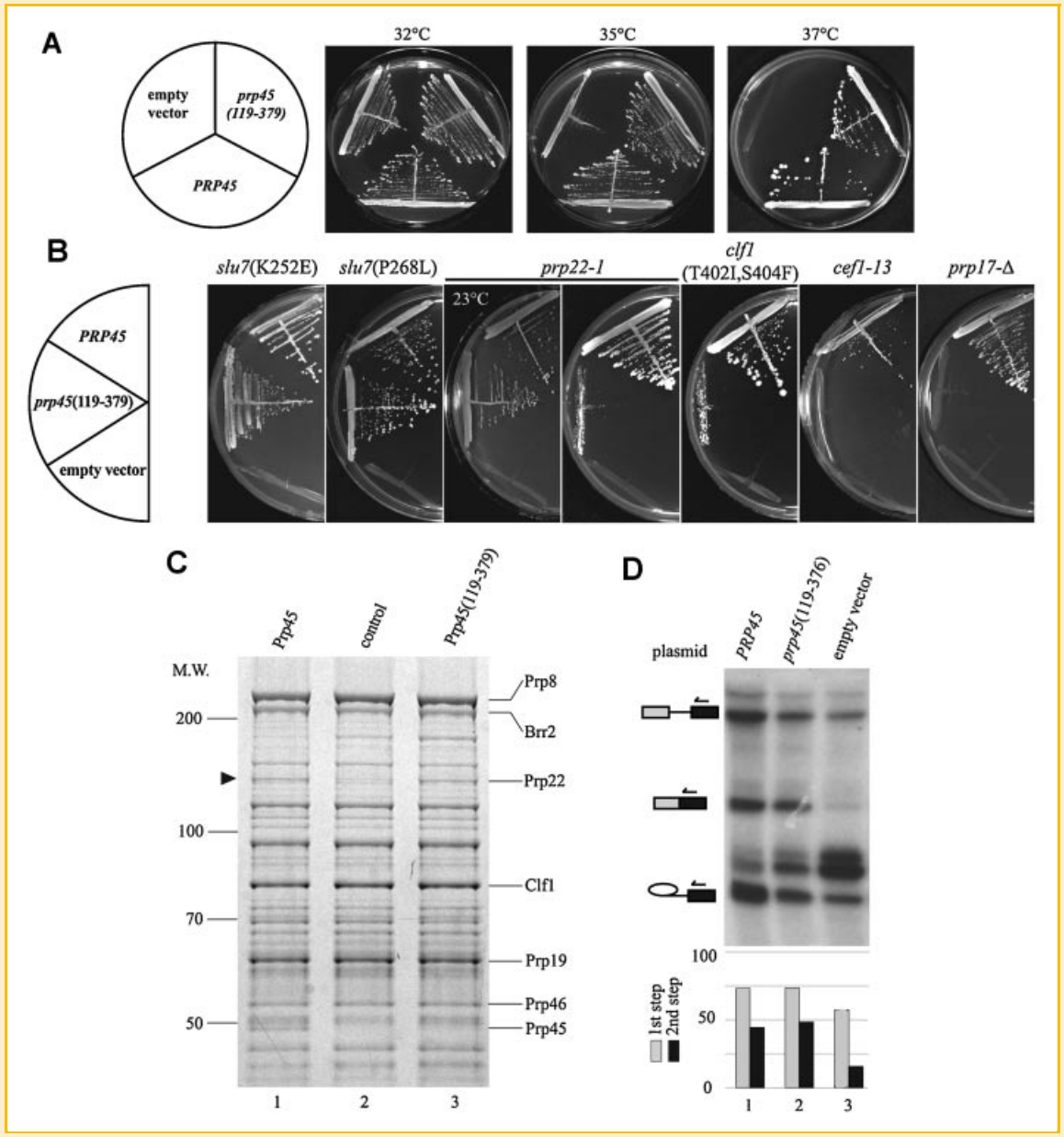

Fig. 6. Prp45(119–379) protein *trans*-complements the *prp45*(1–169) mutation in vivo. A: Prp45(119–379) rescues the temperature sensitive phenotype of *prp45*(1–169) mutation. *prp45*(1–169) cells transformed with the plasmid expressing Prp45(119–379) were cultivated on SD plates at indicated temperatures. Cells harboring the *PRP45* plasmid or empty vector were used as positive or negative controls, respectively. B: Prp45(119–379) suppresses some of the synthetic lethal interactions of *prp45*(1–169). The double mutant strains harboring *prp45*(1–169) and either *prp17*-Δ, *cef1-13*, *clf1*(T402I,S404F), *prp22-1*, *slu7*(P268L), or *slu7*(K252E) mutations depend on Prp45 expressed from the *URA3* plasmid. The cells were transformed with plasmid expressing tagged Prp45(119–379) or Prp45; the empty vector was used as a control. Transformants were tested for growth on 5-FOA plates at 30° or 23°C as indicated. C: Prp45(119–379) restores the content of Prp22 in spliceosomal complexes purified from the *prp45*(1–169) strain. The complexes were isolated using Cwc2-TAP from *prp45*(1–169) cells transformed with plasmid expressing Prp45(119–379) (lane 3). The extracts from the same strain transformed with empty (lane 2) or *PRP45*-harboring plasmid (lane 1) were used as negative and positive control, respectively. The cells were grown in YPD at 23°C; proteins were isolated, separated, stained, and annotated as in Figure 4. D: Prp45(119–379) increases the splicing efficiency of non-consensus 3′ splice site template in *prp45*(1–169) cells. *prp45*(1–169) cells were co-transformed with the plasmid expressing the *ACT1-CUP1* reporter with gAG 3′ss mutation and the plasmid expressing either Prp45 or Prp45(119–379). Empty plasmid served as a control. The primer extension reactions, gel electrophoresis, and quantifications were performed as described in Figure 5.

1999; Ohi et al., 2005], is part of a network of mutual interactions involving Syf1, Syf2, Clf1, and Prp46 [Ben Yehuda et al., 2000; Ohi et al., 2002]. In two-hybrid assay, Clf1 interacts with Prp46, Prp45, as well as Prp22, and Prp45 in turn associates with both Prp22 and Prp46 [Albers et al., 2003]. WD protein Prp17 is required for the efficient completion of the second splicing step [Lindsey-Boltz et al., 2000] and its null allele is synthetically lethal with alleles of *SYF1*, *SYF2*, *CLF1*, *SLU7*, *PRP18*, and *PRP22*, among others [Frank et al.,

1992; Seshadri et al., 1996; Ben Yehuda et al., 2000]. The essential Slu7 factor associates in two-hybrid with Brr2, Prp18, and Prp22, albeit weakly with the latter protein [van Nues and Beggs, 2001]. The Slu7 mutations we identified hit a highly conserved region between arginines 247 and 271, which lies within the essential part of the protein (Fig. 3D). *prp45*(1–169) is not allele specific with respect to the two mutations, reflecting perhaps the fact that both impair a single functionality, such as a binding site.

The novel *prp45*(1–169) SL relationships provide a strong functional evidence for the involvement of Prp45 in the second step spliceosome. Moreover, they corroborate earlier data of two-hybrid interactions of Prp45 [Albers et al., 2003] and its partition in spliceosomal complexes analyzed using a proteomic approach [Ohi et al., 2002].

Prp45 AIDS IN RECRUITING Prp22 TO THE SPLICEOSOME AND AFFECTS THE SPLICING OF NON-CONSENSUS SUBSTRATES

Using artificial *ACT1-CUP1* reporter pre-mRNAs in splicing assays in vivo, we showed that splicing of mutant branch point and 5′ or 3′ splice site templates in *prp45*(1–169) cells is impaired, while splicing of canonical intron is unaffected. The two catalytic steps were affected differentially; while the defects of the branch point mutants BS-C and BS-G were exacerbated only in the 1st step, splicing of the 5′ss A3C and the 3′ss gAG mutants was impaired mainly in the 2nd step (Fig. 5). Using a biochemical approach, we found that Prp22 partition in Cwc2-TAP splicing protein complexes is grossly reduced in the *prp45*(1–169) strain (Fig. 4A). The hypothesis that the defective recruitment of Prp22 is responsible in part for the phenotype of *prp45*(1–169) mutant is further supported by the findings that moderate over expression of Prp22 partly suppresses temperature sensitivity of *prp45*(1–169) strain and that the *prp22* mutations which lead to decreased Prp22 concentration in cells (Fig. 4B,C) are synthetically lethal with *prp45*(1–169). We reason that all these phenotypes reflect missing structural and/or regulatory functions of the C-terminus of Prp45 within the catalytic spliceosome.

Independent lines of evidence suggest a relationship between Prp45 and Prp22: (i) C-terminal part of Prp45 interacts with Prp22 in two hybrid [Albers et al., 2003], (ii) *prp45*(1–169) is synthetically lethal with alleles *prp22*(-158T), *prp22*(-327A), as well as *prp22*(300PPI), and *prp22-1* (Fig. 3 and Table II), (iii) the absence of the C-terminus of Prp45 results in decreased partition of Prp22 in spliceosomal complexes (Fig. 4A), (iv) the expression *in trans* of the C-terminal half of the protein restores the Prp22 stoichiometry (Fig. 6), and (v) the over-expression of Prp22 partly suppresses the ts phenotype of *prp45*(1–169) cells (Fig. 4C). The data suggest that Prp45 is involved in the regulation of Prp22, either indirectly by affecting the 2nd step conformation or directly by binding and regulating the ATPase/translocase. According to recent models [Query and Konarska, 2006], Prp22 destabilizes the 2nd step catalytic conformation and uses ATP to discriminate against aberrant substrates. Prp22 allows only those substrates to splice, which are fast enough to react before the helicase completes its ATP dependent reaction cycle. In addition, as the authors propose, properly bound intermediates could repress Prp22 until after the exon ligation is accomplished and the RNA conformation is changed, boosting Prp22 activity [Mayas et al., 2006]. Similarly, the Prp43 helicase, which acts after the Prp22, requires the interaction with an accessory factor Spp382/Ntr1 for spliceosome binding and proper activity in vivo [Tanaka et al., 2007].

We documented that in addition to *prp45*(1–169), *prp22-1* and *slu7*(P268L) alleles also increase the lariat-exon 2 intermediate/mRNA ratio for the 3′ splice site gAG mutant (Fig. 5C). The synthetic lethality of *prp45*(1–169) and *slu7*(P268L) together with the similarity of their splicing defects with respect to 3′ splice site mutants support the assumption that both proteins cooperate in recruiting Prp22 and/or modulating its activity [see also James et al., 2002]. It has been proposed previously that changes in factors that influence the association of the Prp16 helicase with the spliceosome might result in fidelity changes at the branch site [Burgess and Guthrie, 1993; Villa and Guthrie, 2005]. Similarly, Slu7 and Prp45 might affect 3′ splice site usage fidelity by contributing to the regulation of Prp22 [Mayas et al., 2006 and this study].

Prp45 CAN BE FUNCTIONALLY RECONSTITUTED BY CO-EXPRESSION *IN TRANS*

We showed that Prp45(119–379), which is non-functional when expressed in *prp45*-Δ background, suppressed the *prp45*(1–169) phenotype, including cell division defects, impaired processing of non-canonical introns (Fig. 6D), and decreased levels of Prp22 in Cwc2 pull-downs (Fig. 6C). Prp45 was thus capable of functioning with its parts assembled posttranslationally, similarly to the splicing factors Prp22 and Prp8 [Schneider and Schwer, 2001; Boon et al., 2006]. We assume that the spliceosomal snRNP serves the two Prp45 parts as a scaffold, substituting for the covalent bond, or that the N- and C-terminal parts interact with each other. The latter possibility is supported by the finding that the Prp45 homolog of *S. pombe* Snw1p was capable of a homotypic interaction in a two-hybrid system [Ambrozkova et al., 2001].

In conclusion, the phenotypes and genetic interactions we documented argue for the role of Prp45 in supporting the conformation of the catalytic spliceosome during both steps of splicing. Our findings are in accord with the role of Prp45 as part of NTC and show that C-terminal half of Prp45 contributes structural and/or regulatory features which help the spliceosome in discriminating between canonical and aberrant templates. Accordingly, the phenotypic defects of *prp45*(1–169) cells may be caused by aberrant processing of a responsive group of introns. While the splice site and branch point nucleotides conform to a strict consensus in *S. cerevisiae*, the variations in neighboring sequences as well as in BS-3′ss distances were found to differentially affect spliceosomal performance [Brys and Schwer, 1996; Crotti et al., 2007]. In higher eukaryotes, altered fidelity and efficiency of splicing leads to altered splice site selection. SNW1/SKIP, the Prp45 homolog in human, was shown to affect alternative splice site selection in HIV [Bres et al., 2005]. It is intriguing to speculate that SNW1/SKIP might regulate gene expression by differentially affecting spliceosomal fidelity, possibly in cooperation with the DEAH box helicase HRH1/hPrp22.

ACKNOWLEDGMENTS

The plasmids bearing alleles of splicing factors and the *ACT1-CUP1* constructs used in this study were kindly provided by S-C. Cheng, K. Gould, C. Guthrie, M. Konarska, M. Kupiec, and B. Schwer. The anti-Prp22 antibody was a kind gift of B. Schwer. We thank T. Simonova for the preparation of the strains TSY01 and TSY02, and E. Krellerova for excellent technical assistance. We acknowledge the helpful comments of M. Konarska and the technical support in A. Pichova Lab. This work was supported by the Czech Ministry of Education, Youth and Sports grants MSM0021620858 and LC07032, the Czech Science Foundation grant 204/02/1512, and the Grant Agency of the Charles University grant B170/2005.

REFERENCES

Albers M, Diment A, Muraru M, Russell CS, Beggs JD. 2003. Identification and characterization of Prp45p and Prp46p, essential pre-mRNA splicing factors. RNA 9:138–150.

Ambrozkova M, Puta F, Fukova I, Skruzny M, Brabek J, Folk P. 2001. The fission yeast ortholog of the coregulator SKIP interacts with the small subunit of U2AF. Biochem Biophys Res Commun 284:1148–1154.

Arenas JE, Abelson JN. 1997. Prp43: An RNA helicase-like factor involved in spliceosome disassembly. Proc Natl Acad Sci USA 94:11798–11802.

Aronova A, Bacikova D, Crotti LB, Horowitz DS, Schwer B. 2007. Functional interactions between Prp8, Prp18, Slu7, and U5 snRNA during the second step of pre-mRNA splicing. RNA 13:1437–1444.

Bassler J, Grandi P, Gadal O, Lessmann T, Petfalski E, Tollervey D, Lechner J, Hurt E. 2001. Identification of a 60S preribosomal particle that is closely linked to nuclear export. Mol Cell 8:517–529.

Ben Yehuda S, Dix I, Russell CS, McGarvey M, Beggs JD, Kupiec M. 2000. Genetic and physical interactions between factors involved in both cell cycle progression and pre-mRNA splicing in Saccharomyces cerevisiae. Genetics 156:1503–1517.

Bessonov S, Anokhina M, Will CL, Urlaub H, Luhrmann R. 2008. Isolation of an active step I spliceosome and composition of its RNP core. Nature 452:846–850.

Boon KL, Norman CM, Grainger RJ, Newman AJ, Beggs JD. 2006. Prp8p dissection reveals domain structure and protein interaction sites. RNA 12:198–205.

Bres V, Gomes N, Pickle L, Jones KA. 2005. A human splicing factor, SKIP, associates with P-TEFb and enhances transcription elongation by HIV-1 Tat. Genes Dev 19:1211–1226.

Brys A, Schwer B. 1996. Requirement for SLU7 in yeast pre-mRNA splicing is dictated by the distance between the branchpoint and the 3' splice site. RNA 2:707–717.

Burgess SM, Guthrie C. 1993. A mechanism to enhance mRNA splicing fidelity: The RNA-dependent ATPase Prp16 governs usage of a discard pathway for aberrant lariat intermediates. Cell 73:1377–1391.

Burns CG, Ohi R, Mehta S, O'Toole ET, Winey M, Clark TA, Sugnet CW, Ares M, Jr., Gould KL. 2002. Removal of a single alpha-tubulin gene intron suppresses cell cycle arrest phenotypes of splicing factor mutations in Saccharomyces cerevisiae. Mol Cell Biol 22:801–815.

Chan SP, Cheng SC. 2005. The Prp19-associated complex is required for specifying interactions of U5 and U6 with pre-mRNA during spliceosome activation. J Biol Chem 280:31190–31199.

Chawla G, Sapra AK, Surana U, Vijayraghavan U. 2003. Dependence of pre-mRNA introns on PRP17, a non-essential splicing factor: Implications for efficient progression through cell cycle transitions. Nucleic Acids Res 31:2333–2343.

Crotti LB, Bacikova D, Horowitz DS. 2007. The Prp18 protein stabilizes the interaction of both exons with the U5 snRNA during the second step of pre-mRNA splicing. Genes Dev 21:1204–1216.

Dahan O, Kupiec M. 2002. Mutations in genes of Saccharomyces cerevisiae encoding pre-mRNA splicing factors cause cell cycle arrest through activation of the spindle checkpoint. Nucleic Acids Res 30:4361–4370.

Frank D, Patterson B, Guthrie C. 1992. Synthetic lethal mutations suggest interactions between U5 small nuclear RNA and four proteins required for the second step of splicing. Mol Cell Biol 12:5197–5205.

Gavin AC, Bosche M, Krause R, Grandi P, Marzioch M, Bauer A, Schultz J, Rick JM, Michon AM, Cruciat CM, Remor M, Hofert C, Schelder M, Brajenovic M, Ruffner H, Merino A, Klein K, Hudak M, Dickson D, Rudi T, Gnau V, Bauch A, Bastuck S, Huhse B, Leutwein C, Heurtier MA, Copley RR, Edelmann A, Querfurth E, Rybin V, Drewes G, Raida M, Bouwmeester T, Bork P, Seraphin B, Kuster B, Neubauer G, Superti-Furga G. 2002. Functional organization of the yeast proteome by systematic analysis of protein complexes. Nature 415:141–147.

Ghaemmaghami S, Huh WK, Bower K, Howson RW, Belle A, Dephoure N, O'Shea EK, Weissman JS. 2003. Global analysis of protein expression in yeast. Nature 425:737–741.

Golemis EA, Gyuris J, Brent R. 1996. Interaction trap/two-hybrid system to identify interacting proteins. In: Ausubel FM, Brent R, Kingston RE, Moore DD, Seidman JD, Smith JA, Struhl K, editors. Current protocols in molecular biology, Unit 20.1. New York: Wiley.

Huh WK, Falvo JV, Gerke LC, Carroll AS, Howson RW, Weissman JS, O'Shea EK. 2003. Global analysis of protein localization in budding yeast. Nature 425:686–691.

James SA, Turner W, Schwer B. 2002. How Slu7 and Prp18 cooperate in the second step of yeast pre-mRNA splicing. RNA 8:1068–1077.

Juneau K, Palm C, Miranda M, Davis RW. 2007. High-density yeast-tiling array reveals previously undiscovered introns and extensive regulation of meiotic splicing. Proc Natl Acad Sci USA 104:1522–1527.

Jurica MS, Moore MJ. 2003. Pre-mRNA splicing: Awash in a sea of proteins. Mol Cell 12:5–14.

Kabani M, Michot K, Boschiero C, Werner M. 2005. Anc1 interacts with the catalytic subunits of the general transcription factors TFIID and TFIIF, the chromatin remodeling complexes RSC and INO80, and the histone acetyltransferase complex NuA3. Biochem Biophys Res Commun 332:398–403.

Konarska MM, Vilardell J, Query CC. 2006. Repositioning of the reaction intermediate within the catalytic center of the spliceosome. Mol Cell 21:543–553.

Koren A, Ben Aroya S, Steinlauf R, Kupiec M. 2003. Pitfalls of the synthetic lethality screen in Saccharomyces cerevisiae: An improved design. Curr Genet 43:62–69.

Korolyev E, Steinberg-Neifach O, Eshel D. 2005. Mutations in the yeast kinesin-like Cin8p are alleviated by osmotic support. FEMS Microbiol Lett 244:379–383.

Leong GM, Subramaniam N, Figueroa J, Flanagan JL, Hayman MJ, Eisman JA, Kouzmenko AP. 2001. Ski-interacting protein interacts with Smad proteins to augment transforming growth factor-beta-dependent transcription. J Biol Chem 276:18243–18248.

Lesser CF, Guthrie C. 1993. Mutational analysis of pre-mRNA splicing in Saccharomyces cerevisiae using a sensitive new reporter gene, CUP1. Genetics 133:851–863.

Lindsey-Boltz LA, Chawla G, Srinivasan N, Vijayraghavan U, Garcia-Blanco MA. 2000. The carboxy terminal WD domain of the pre-mRNA splicing factor Prp17p is critical for function. RNA 6:1289–1305.

Liu L, Query CC, Konarska MM. 2007. Opposing classes of prp8 alleles modulate the transition between the catalytic steps of pre-mRNA splicing. Nat Struct Mol Biol 14:519–526.

Longtine MS, McKenzie A III, Demarini DJ, Shah NG, Wach A, Brachat A, Philippsen P, Pringle JR. 1998. Additional modules for versatile and eco-

nomical PCR-based gene deletion and modification in Saccharomyces cerevisiae. Yeast 14:953–961.

Lopez de Heredia M, Jansen RP. 2004. RNA integrity as a quality indicator during the first steps of RNP purifications: A comparison of yeast lysis methods. BMC Biochem 5:14.

Makarov EM, Makarova OV, Urlaub H, Gentzel M, Will CL, Wilm M, Luhrmann R. 2002. Small nuclear ribonucleoprotein remodeling during catalytic activation of the spliceosome. Science 298:2205–2208.

Martinkova K, Lebduska P, Skruzny M, Folk P, Puta F. 2002. Functional mapping of Saccharomyces cerevisiae Prp45 identifies the SNW domain as essential for viability. J Biochem (Tokyo) 132:557–563.

Mayas RM, Maita H, Staley JP. 2006. Exon ligation is proofread by the DExD/H-box ATPase Prp22p. Nat Struct Mol Biol 13:482–490.

Ohi MD, Gould KL. 2002. Characterization of interactions among the Cef1p-Prp19p-associated splicing complex. RNA 8:798–815.

Ohi MD, Link AJ, Ren L, Jennings JL, McDonald WH, Gould KL. 2002. Proteomics analysis reveals stable multiprotein complexes in both fission and budding yeasts containing Myb-related Cdc5p/Cef1p, novel pre-mRNA splicing factors, and snRNAs. Mol Cell Biol 22:2011–2024.

Ohi MD, Vander Kooi CW, Rosenberg JA, Ren L, Hirsch JP, Chazin WJ, Walz T, Gould KL. 2005. Structural and functional analysis of essential pre-mRNA splicing factor Prp19p. Mol Cell Biol 25:451–460.

Pleiss JA, Whitworth GB, Bergkessel M, Guthrie C. 2007a. Rapid, transcript-specific changes in splicing in response to environmental stress. Mol Cell 27:928–937.

Pleiss JA, Whitworth GB, Bergkessel M, Guthrie C. 2007b. Transcript specificity in yeast pre-mRNA splicing revealed by mutations in core spliceosomal components. PLoS Biol 5:e90.

Prathapam T, Kuhne C, Banks L. 2002. Skip interacts with the retinoblastoma tumor suppressor and inhibits its transcriptional repression activity. Nucleic Acids Res 30:5261–5268.

Preker PJ, Kim KS, Guthrie C. 2002. Expression of the essential mRNA export factor Yra1p is autoregulated by a splicing-dependent mechanism. RNA 8:969–980.

Puig O, Caspary F, Rigaut G, Rutz B, Bouveret E, Bragado-Nilsson E, Wilm M, Seraphin B. 2001. The tandem affinity purification (TAP) method: A general procedure of protein complex purification. Methods 24:218–229.

Query CC, Konarska MM. 2006. Splicing fidelity revisited. Nat Struct Mol Biol 13:472–474.

Racki WJ, Becam AM, Nasr F, Herbert CJ. 2000. Cbk1p, a protein similar to the human myotonic dystrophy kinase, is essential for normal morphogenesis in Saccharomyces cerevisiae. EMBO J 19:4524–4532.

Reed SI, Hadwiger JA, Richardson HE, Wittenberg C. 1989. Analysis of the Cdc28 protein kinase complex by dosage suppression. J Cell Sci Suppl 12:29–37.

Schneider S, Schwer B. 2001. Functional domains of the yeast splicing factor Prp22p. J Biol Chem 276:21184–21191.

Schwer B. 2008. A conformational rearrangement in the spliceosome sets the stage for Prp22-dependent mRNA release. Mol Cell 30:743–754.

Schwer B, Gross CH. 1998. Prp22, a DExH-box RNA helicase, plays two distinct roles in yeast pre-mRNA splicing. EMBO J 17:2086–2094.

Seshadri V, Vaidya VC, Vijayraghavan U. 1996. Genetic studies of the PRP17 gene of Saccharomyces cerevisiae: A domain essential for function maps to a nonconserved region of the protein. Genetics 143:45–55.

Shea JE, Toyn JH, Johnston LH. 1994. The budding yeast U5 snRNP Prp8 is a highly conserved protein which links RNA splicing with cell cycle progression. Nucleic Acids Res 22:5555–5564.

Shen H, Green MR. 2006. RS domains contact splicing signals and promote splicing by a common mechanism in yeast through humans. Genes Dev 20:1755–1765.

Siatecka M, Reyes JL, Konarska MM. 1999. Functional interactions of Prp8 with both splice sites at the spliceosomal catalytic center. Genes Dev 13:1983–1993.

Smith DJ, Query CC, Konarska MM. 2007. trans-splicing to spliceosomal U2 snRNA suggests disruption of branch site-U2 pairing during pre-mRNA splicing. Mol Cell 26:883–890.

Stevens SW, Ryan DE, Ge HY, Moore RE, Young MK, Lee TD, Abelson J. 2002. Composition and functional characterization of the yeast spliceosomal penta-snRNP. Mol Cell 9:31–44.

Tanaka N, Aronova A, Schwer B. 2007. Ntr1 activates the Prp43 helicase to trigger release of lariat-intron from the spliceosome. Genes Dev 21:2312–2325.

Tarn WY, Hsu CH, Huang KT, Chen HR, Kao HY, Lee KR, Cheng SC. 1994. Functional association of essential splicing factor(s) with PRP19 in a protein complex. EMBO J 13:2421–2431.

Thomas BJ, Rothstein R. 1989. Elevated recombination rates in transcriptionally active DNA. Cell 56:619–630.

Thompson JD, Higgins DG, Gibson TJ. 1994. CLUSTAL W: Improving the sensitivity of progressive multiple sequence alignment through sequence weighting, position-specific gap penalties and weight matrix choice. Nucleic Acids Res 22:4673–4680.

Tsai WY, Chow YT, Chen HR, Huang KT, Hong RI, Jan SP, Kuo NY, Tsao TY, Chen CH, Cheng SC. 1999. Cef1p is a component of the Prp19p-associated complex and essential for pre-mRNA splicing. J Biol Chem 274:9455–9462.

Vaisman N, Tsouladze A, Robzyk K, Ben Yehuda S, Kupiec M, Kassir Y. 1995. The role of Saccharomyces cerevisiae Cdc40p in DNA replication and mitotic spindle formation and/or maintenance. Mol Gen Genet 247:123–136.

Valadkhan S. 2005. snRNAs as the catalysts of pre-mRNA splicing. Curr Opin Chem Biol 9:603–608.

van Nues RW, Beggs JD. 2001. Functional contacts with a range of splicing proteins suggest a central role for Brr2p in the dynamic control of the order of events in spliceosomes of Saccharomyces cerevisiae. Genetics 157:1451–1467.

Vijayraghavan U, Company M, Abelson J. 1989. Isolation and characterization of pre-mRNA splicing mutants of Saccharomyces cerevisiae. Genes Dev 3:1206–1216.

Villa T, Guthrie C. 2005. The Isy1p component of the NineTeen complex interacts with the ATPase Prp16p to regulate the fidelity of pre-mRNA splicing. Genes Dev 19:1894–1904.

Vincent K, Wang Q, Jay S, Hobbs K, Rymond BC. 2003. Genetic interactions with CLF1 identify additional pre-mRNA splicing factors and a link between activators of yeast vesicular transport and splicing. Genetics 164:895–907.

Wang Q, Hobbs K, Lynn B, Rymond BC. 2003. The Clf1p splicing factor promotes spliceosome assembly through N-terminal tetratricopeptide repeat contacts. J Biol Chem 278:7875–7883.

Will CL, Luhrmann R, 2006. Spliceosome structure and function. In: Gesteland RF, Cech TR, Atkins JF, editors. The RNA world. New York: Cold Spring Harbor Laboratory Press. pp. 369–400.

Zhang X, Schwer B. 1997. Functional and physical interaction between the yeast splicing factors Slu7 and Prp18. Nucleic Acids Res 25:2146–2152.

Zhang C, Baudino TA, Dowd DR, Tokumaru H, Wang W, MacDonald PN. 2001. Ternary complexes and cooperative interplay between NCoA-62/Ski-interacting protein and steroid receptor coactivators in vitamin D receptor-mediated transcription. J Biol Chem 276:40614–40620.

Zhang C, Dowd DR, Staal A, Gu C, Lian JB, van Wijnen AJ, Stein GS, MacDonald PN. 2003. Nuclear coactivator-62 kDa/Ski-interacting protein is a nuclear matrix-associated coactivator that may couple vitamin D receptor-mediated transcription and RNA splicing. J Biol Chem 278:35325–35336.

Zhou S, Fujimuro M, Hsieh JJ, Chen L, Miyamoto A, Weinmaster G, Hayward SD. 2000. SKIP, a CBF1-associated protein, interacts with the ankyrin repeat domain of NotchIC To facilitate NotchIC function. Mol Cell Biol 20:2400–2410.